

Improving r -process calculations for the rare-earth abundance peak via mass measurements at JYFLTRAP

M. Vilen,^{1,*} J.M. Kelly,^{2,†} A. Kankainen,¹ M. Brodeur,² A. Aprahamian,² L. Canete,¹ T. Eronen,¹ A. Jokinen,¹ T. Kuta,² I.D. Moore,¹ M.R. Mumpower,^{2,3} D.A. Nesterenko,¹ H. Penttälä,¹ I. Pohjalainen,¹ W.S. Porter,² S. Rinta-Antila,¹ R. Surman,² A. Voss,¹ and J. Äystö¹

¹*University of Jyväskylä, P.O. Box 35, FI-40014 University of Jyväskylä, Finland*

²*University of Notre Dame, Notre Dame, Indiana 46556, USA*

³*Theory Division, Los Alamos National Lab, Los Alamos, New Mexico 87544, USA*

(Dated: December 14, 2017)

The rare-earth peak in the r -process abundance pattern depends sensitively on both the astrophysical conditions and subtle changes in nuclear structure in the region. This work takes an important step elucidating the nuclear structure and reducing the uncertainties in r -process calculations via precise atomic mass measurements at the JYFLTRAP double Penning trap. ^{158}Nd , $^{160,162}\text{Pm}$, and $^{164-166}\text{Gd}$ have been measured for the first time and the precisions for ^{156}Nd , ^{158}Pm , $^{162,163}\text{Eu}$, ^{163}Gd , and ^{164}Tb have been improved considerably. The effect of the new mass values on the calculated r -process abundances has been studied for a neutron star merger scenario. Substantial changes in the abundances in the lanthanide region relevant for optical observations from neutron star mergers have been found. These are mainly due to lower neutron separation energies at $N = 98, 100$ and 102 leading to smaller odd-even staggering than predicted by theoretical mass models. Two-neutron separation energies exhibit changes in their slopes after $N = 96$ for the Nd ($Z = 60$) and after $N = 100$ for the Gd ($Z = 64$) isotopes but they do not support the existence of a subshell closure at $N = 100$. Further studies are anticipated to shed light on the underlying physics affecting the binding energies, and eventually, the r -process abundances.

PACS numbers: 21.10.Dr, 26.30.Hj, 27.70.+q

The astrophysical rapid neutron capture process (r -process) [1–3] is responsible for the production of around half of the elements heavier than iron. The r -process and its astrophysical site has driven research not only in nuclear astrophysics, but in multiple fields, including nuclear structure [4, 5] and theory [6, 7], accelerator mass spectrometry [8] and observational astronomy [9, 10]. Various astrophysical sites have been proposed over the years, e.g. neutrino-driven winds from the remnants of core-collapse supernovae [3, 11], magnetohydrodynamic supernovae [12], and neutron star mergers [13–18]. The recent, seminal multi-messenger observations of a neutron star merger [19], namely the gravitational waves from GW170817 [20] followed by a kilonova (AT 2017 gfo) powered by the radioactive decay of r -process nuclei synthesized in the ejecta [21, 22], provide direct evidence that the r -process takes place in neutron star mergers. For the first time, this allows the testing of r -process abundance models using an unpolluted sample [23]. Hence, there is now a strong impetus to have accurate nuclear physics inputs to ensure the reliability of the abundance calculations. With their high opacity, lanthanides play a central role in the optical observations and diagnostics of heavy r -process ejecta from such mergers [24, 25]. In this Letter, we present results for nuclear binding energies that affect the calculated r -process abundances of lanthanides in the rare-earth region.

Because the r -process path traverses uncharted and largely inaccessible regions of the chart of nuclides, there is a scarcity of experimental information with which to constrain the astrophysical calculations. Detailed r -process sensitivity studies performed in recent years [26–29] have shown that among the various quantities entering into their calculations, e.g. neutron-capture and photodisintegration rates, beta-decay half-lives, and beta-delayed neutron emission and fission probabilities, it is the quantities most strongly derivative of nuclear mass, namely binding energies, that proved to be the most sensitive [28]. However, the masses of the most relevant r -process nuclei have never been measured, leaving nuclear abundance calculations to rely on theoretical mass models such as FRDM12 [30], HFB-24 [31], Duflo-Zuker [32] or Skyrme energy-density functionals [7] for these critical inputs. While the mass models agree closely with one another in regions with existing measurements, they diverge strongly in the absence of such empirical data, which has profound impacts on abundance peak formation simulations [28].

The formation of the rare-earth abundance peak is very sensitive to nuclear structure in the neutron-rich rare-earth region. A confluence of nuclear deformation and β -decay properties peculiar to nuclei surrounding $A = 165$ is understood to create a funneling effect that draws the nuclei towards the peak as neutron captures dwindle and existing radionuclides decay towards stability [34, 35]. Furthermore, fission recycling is believed to augment this process as the fragments of heavier, unstable nuclides beyond the third ($A \approx 195$) peak could cycle back into

* markus.k.vilen@student.jyu.fi

† jkelly27@nd.edu

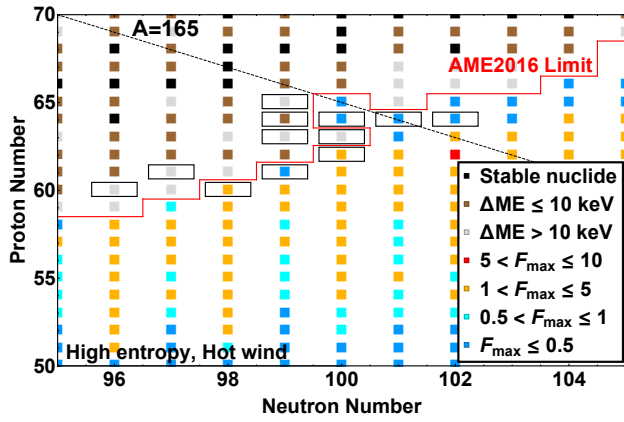


FIG. 1: (Color online) The nuclei studied in this work (surrounded with black boxes) and the r -process impact factors, F_{max} (see Ref. [28]), in a high entropy, hot wind astrophysical scenario, using the Atomic Mass Evaluation 2016 (AME16) mass values [33] and the FRDM12 mass model [30].

the rare-earth region [17, 35, 36]. Yet even these late-stage processes show marked differences depending on astrophysical conditions [29]. Fortunately, the rare-earth abundances are some of the most precisely known in the solar system and in metal-poor stars [37]. Observational information on the rare-earth abundances can even be used to investigate nuclear structure far from stability via the reverse-engineering of a more accurate mass model [29].

The rare-earth region, located in the midshell bounded by $Z = 50 - 82$ and $N = 82 - 126$, incorporates several interesting nuclear structure features that can affect the r process. A surge of research was triggered by the discovery of the onset of strong prolate deformation at $N = 88 - 90$ in the 1950s [38, 39]. Proton-neutron interactions enhanced in nuclei with approximately equal numbers of valence protons and neutrons have been found to play a key role in the evolution of nuclear structure and collectivity in this region [40–42]. A local minimum in the $E(2^+)$ energies and a local maximum of moment of inertia have been observed for the Gd isotopes at $N = 98$ via γ -ray spectroscopy at Gammasphere [43]. Jones et al. [43] also found ^{164}Gd ($N = 100$) to be more rigid and to show less stretching than ^{162}Gd , suggesting a possible change in structure. Recently, γ -ray spectroscopy on ^{164}Sm and ^{166}Gd with EURICA at RIBF revealed an increase in the $E(2^+)$ and $E(4^+)$ energies at $N = 100$ in comparison with the $N = 98$ cases for Gd and Sm isotopes, supporting an implied sub-shell closure at $N = 100$ proffered by the Hartree-Fock calculations of [44]. Interestingly, recent half-life measurements performed at RIKEN [45] did not find any supporting evidence for the $N = 100$ subshell closure. Additionally the systematics of the new K isomers found in the neutron-rich $N = 100$ isotones ^{162}Sm , ^{163}Eu , and ^{164}Gd at RIKEN could be explained without the predicted $N = 100$ shell gap [46].

Although information on beta-decay half-lives [45] and level structures [43, 47] of rare-earth nuclei has increased substantially in recent years, nuclear binding energies - i.e. masses - have not been pursued so intensively. The Canadian Penning Trap (CPT) has explored some rare-earth nuclei in the past [48], and some Q_β measurements have been performed using a total absorption Clover detector [49]. In this Letter we present the first mass measurements of several rare-earth nuclei close to $N = 100$ of significance for the astrophysical r process, while providing further information on the nuclear structure which is of direct relevance for the r -process.

The studied neutron-rich rare-earth nuclei (see Fig. 1) were produced at the Ion Guide Isotope Separator On-Line (IGISOL) facility [50], employing a 25 MeV, 10 – 15 μA proton beam impinging on a 15 mg/cm²-thick natural uranium target. The fission fragments were thermalized in helium buffer gas and extracted from the gas cell with a typical charge state of $q = +e$ by a radio-frequency sextupole ion guide [51]. Subsequently, the ions were accelerated to 30 keV before mass-separation with a dipole magnet. The continuous beam was cooled and bunched in a radio-frequency quadrupole cooler-buncher (RFQ) [52] prior to injection into the double Penning trap mass spectrometer, JYFLTRAP [53]. Isobarically pure ion samples were prepared in the purification trap via the mass-selective buffer gas cooling method [54]. For ^{156}Nd , ^{158}Pm , ^{162}Sm , $^{162-163}\text{Eu}$, $^{163-166}\text{Gd}$ and ^{164}Tb , an additional cleaning phase employing dipolar Ramsey excitations [55] in the second trap was required. The mass measurements were performed by determining the cyclotron frequency, $\nu_c = qB/(2\pi m)$, for an ion with mass m and charge q in a magnetic field B using the time-of-flight ion-cyclotron resonance method (TOF-ICR) [56, 57] (see Fig. 2). A 400-ms quadrupolar excitation scheme was applied for ^{158}Nd and ^{160}Pm . To more accurately determine the frequency, separated oscillatory fields [58, 59] with excitation patterns of 25-350-25 ms (On-Off-On) and 25-750-25 ms (On-Off-On) were applied for ^{156}Nd , ^{158}Pm , ^{162}Sm , $^{162-163}\text{Eu}$, $^{163-166}\text{Gd}$, and ^{164}Tb , and for ^{158}Pm , respectively.

The magnetic field strength was precisely determined by interleaving measurements of a well-known reference ion ($\nu_{c,ref}$) just before and after an ion of interest (ν_c). The mass ratios and atomic masses were then calculated from the ratio of frequencies $r = \nu_{c,ref}/\nu_c$, which equals the ratio of masses. Data analysis followed the procedure described e.g. in Refs. [53, 60]. Temporal fluctuations of the B -field, $\delta_B(\nu_{ref})/\nu_{ref} = \Delta t \cdot 8.18 \cdot 10^{-12}/\text{min}$ [61], where Δt is the time between consecutive reference measurements, and a mass-dependent uncertainty $\delta_m(r)/r = \Delta m \cdot 2.2(6) \cdot 10^{-10}/u$, determined soon after the experiment, were taken into account.

The measured frequency ratios and the corresponding mass-excess values are presented in Table I. Six of the twelve isotopes, namely ^{158}Nd , ^{160}Pm , ^{162}Sm , $^{164-166}\text{Gd}$, were measured for the first time. The precision of the mass-excess values have been improved considerably for

TABLE I: Frequency ratios (r) and mass-excess values (ME) determined in this work with JYFLTRAP compared with AME16 [33]. All measurements were done with singly-charged ions. The reference masses, ^{136}Xe , ^{158}Gd , ^{163}Dy , and ^{171}Yb , were adopted from AME16, and # signs indicate extrapolated values therein.

| Isotope | Reference | $ME_{REF}(\text{keV})$ | $r = \nu_{c,ref}/\nu_c$ | $ME_{JYFL}(\text{keV})$ | $ME_{AME16}(\text{keV})$ | $\Delta ME_{JYFL-AME16}(\text{keV})$ |
|-------------------|-------------------|------------------------|--------------------------------|-------------------------|--------------------------|--------------------------------------|
| ^{156}Nd | ^{136}Xe | -86429.159(7) | 1.147 366 924(19) | -60210(2) | -60470(200) | 260(200) |
| ^{158}Nd | ^{136}Xe | -86429.159(7) | 1.162 132 772(290) | -53897(37) | -54060(200)# | 160(200)# |
| ^{158}Pm | ^{158}Gd | -70689.5(12) | 1.000 078 752(9) | -59104(2) | -59089(13) | -15(13) |
| ^{160}Pm | ^{136}Xe | -86429.159(7) | 1.176 857 014(130) | -52851(16) | -53000(200)# | 149(201)# |
| ^{162}Sm | ^{136}Xe | -86429.159(7) | 1.191 560 914(39) | -54381(5) | -54530(200)# | 149(200)# |
| ^{162}Eu | ^{136}Xe | -86429.159(7) | 1.191 527 132(28) | -58658(4) | -58700(40) | 42(40) |
| ^{163}Eu | ^{163}Dy | -66381.2(8) | 1.000 065 633(23) | -56420(4) | -56480(70) | 60(70) |
| ^{163}Gd | ^{163}Dy | -66381.2(8) | 1.000 034 135(22) | -61200(4) ^a | -61314(8) | 114(9) |
| ^{164}Gd | ^{171}Yb | -59306.810(13) | 0.959 046 522(14) | -59694(3) | -59770(100)# | 76(100)# |
| ^{165}Gd | ^{171}Yb | -59306.810(13) | 1.058 489 243(23) ^b | -56522(4) | -56450(120)# | -72(120)# |
| ^{166}Gd | ^{136}Xe | -86429.159(7) | 1.220 992 828(29) | -54387(4) | -54530(200)# | 143(200)# |
| ^{164}Tb | ^{171}Yb | -59306.810(13) | 0.959 031 473(21) | -62090(4) | -62080(100) | -10(100) |

^a Assuming the measured state is the isomer at 137.8 keV [49], the ground-state mass is $-61338(4)$ keV.

^b Measured as $^{165}\text{Gd}^{16}\text{O}$.

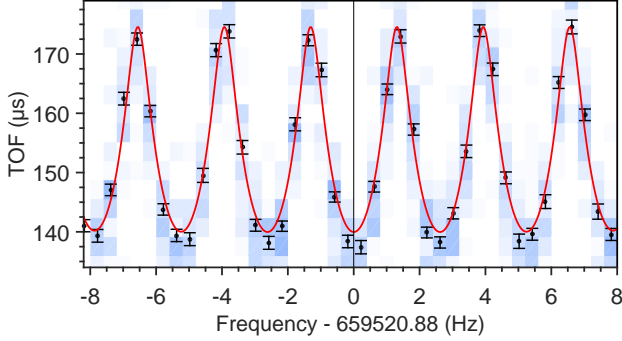


FIG. 2: (Color online) An example of a time-of-flight spectrum for $^{163}\text{Eu}^+$. Background shading indicates the total number of ions, where darker shading indicates more ions.

all studied isotopes. The new values are in agreement with the extrapolated values of the AME16 [33] but the extrapolations seem to have generally overestimated the nuclear binding energies by about 150 keV in this region.

Most of the previously known mass values were based on β -decay Q -value measurements, such as ^{156}Nd [62], $^{162,163}\text{Eu}$ [49], and ^{164}Tb [63]. Although the Q_β values yield lower mass values than the present Penning trap measurement, only ^{156}Nd [62] deviates by more than 1σ from this work. In fact, it has been suggested [64] that based on the trends in the mass surface, ^{156}Nd might be 70 keV less bound than the value derived from the β -decay endpoint measurement [62].

Two of the studied isotopes, ^{158}Pm and ^{163}Gd , have been measured by the Canadian Penning trap [48]. While the results for ^{158}Pm agree within 1σ , they deviate considerably in the case of ^{163}Gd . Interestingly, a new long-lived ($T_{1/2} = 23.5(10)\text{s}$) isomeric state at 137.8 keV in ^{163}Gd was recently discovered [49]. The unusually large

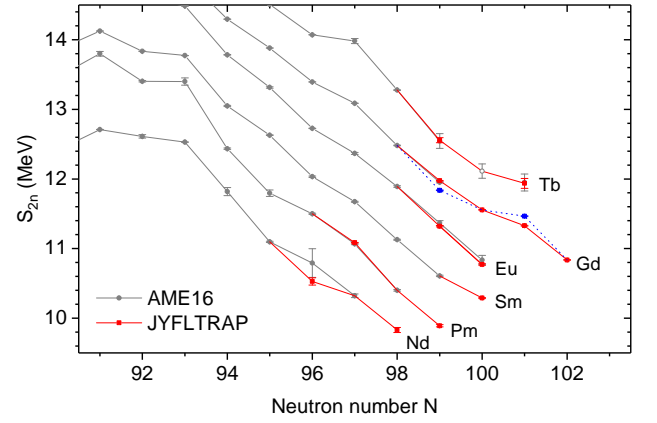


FIG. 3: (Color online) Two-neutron separation energies S_{2n} from this work (red) together with the experimental (solid gray circles) values and an extrapolated value for ^{165}Tb (open gray circle) from AME16 [33]. The dashed blue lines indicate the values assuming the ground state of ^{163}Gd was measured in this work.

discrepancy between this work and CPT [48] could be understood if the proton-induced fission on ^{nat}U at IGISOL had predominantly populated the isomeric state of ^{163}Gd . Assuming we measured the first isomeric state, our corrected mass-excess value differs from CPT by 24(9) keV.

Nuclear structure far from stability can be probed via two-neutron separation energies [65]. They usually exhibit smooth trends except at shell closures or when there is a change in the nuclear structure, such as the shape change in the $N = 60$ region [66]. Figure 3 shows the S_{2n} values determined in this work compared with the values from AME16 [33]. The new S_{2n} values cause a change in the slope after $N = 100$ for the Gd isotopes. A similar effect is also observed for Tb at $N = 100$ and after $N = 96$ for the Nd ($Z = 60$) chain. Incidentally, a local maximum

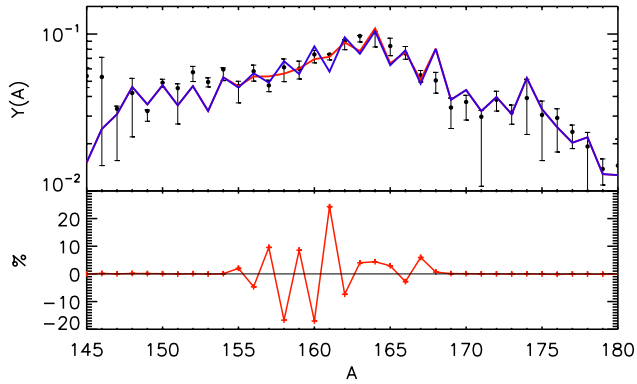


FIG. 4: (Color online) Top: Calculated r -process abundances in the rare-earth region and the solar r -process abundances (black circles). The blue line indicates results using the AME16 [33] + FRDM12 [30] masses, while the red line incorporates the new masses measured in this work. Bottom: Change, in percent, of the abundance pattern as a result of using the atomic masses from this work.

is seen in the $E(2^+)$ energies at $N = 100$ for Gd and Dy. The $E(4^+)/E(2^+)$ ratios are ≈ 3.3 around $N = 100$ compatible with a rigid rotor. The prolate quadrupole deformation is predicted to reach a local maximum for the Gd isotopes at around $N = 101 - 103$ where $\beta_2 \approx 0.31$ [30]. Finally, based on the new mass values from this work, the experimental two-neutron shell-gap energies for $N = 100$ are rather low (< 1 MeV) down to Gd ($Z = 64$), and do not support the proposed subshell gap at $N = 100$ [44, 67, 68].

We also compared the experimental S_{2n} values to the predictions from various mass models commonly used in r -process calculations, such as FRDM12 [30], Dufflo-Zuker [32], and HFB-24 [31]. These models predict a rather smooth behavior for the S_{2n} values in the region of interest and none of them suggest changes in the slope in contrast to those observed in this work. The used mass models seem to overestimate S_{2n} values at $N = 99$ and 100 by around 0.3 MeV for the studied isotopic chains.

The impact of the new mass values on the r -process was studied for several different neutron star merger trajectories, which all yielded similar abundance patterns. Our r -process calculations proceed as in [28] and include fission recycling. We choose a simple asymmetric split [29] for the fission product distributions so that fission products fall into the $A \sim 130$ region and the rare earth peak forms entirely via the dynamical formation mechanism of [34, 35]. For our r -process calculations, masses and relevant Q -values not measured in this work were supplemented with data from AME16 or calculated values from FRDM12. Branching ratios and β -decay half-lives were taken from NUBASE 2016 [69] or from Ref. [70]. The neutron-capture rates were calculated with the commonly used TALYS code [71] us-

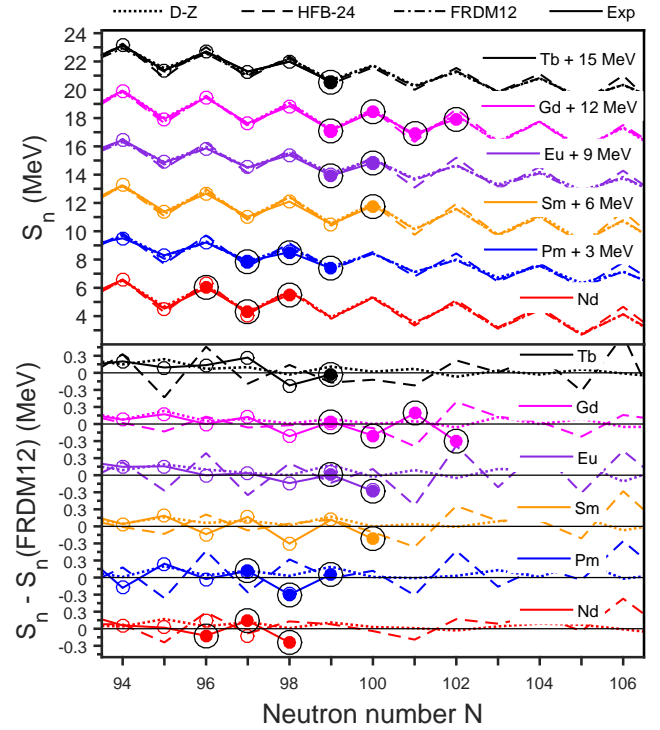


FIG. 5: (Color online) Top: Experimental neutron separation energies compared with the Dufflo-Zuker [32], HFB-24 [31], and FRDM12 [30] models. Energies from this work are highlighted with big circles. Bottom: differences to FRDM12.

ing the revised mass data set described above. The calculated abundance pattern $Y(A)$ in Fig. 4 is based on a neutron star merger trajectory from [72], where the blue line shows the abundance using AME16 [33] and FRDM12 [30] masses and the red line makes use of the new masses from Table I. As shown in Fig. 4, changes in the abundance pattern of up to 24% are observed. Clearly, a better agreement with the solar abundance pattern is obtained including our new mass values ($\chi^2=10.7$) than with the AME16 and FRDM12 values used as a baseline ($\chi^2=18.9$). Here, χ^2 has been defined as $\chi^2 = \sum ((Y(A)_{solar} - Y(A)_{calc.})/\sigma(Y(A)_{solar}))^2$ with $\sigma(Y(A)_{solar})$ being the uncertainty of the solar abundances and the sum being over the mass number region ($A = 154 - 168$) affected by the measurements reported in this Letter.

The nuclei studied in this work are populated at late times in the r -process, after $(n, \gamma) - (\gamma, n)$ equilibrium has failed. At this stage, the material is decaying back toward stability and the fine details of the final abundance pattern are set through a competition between neutron capture and β -decay. Although the present work provides more accurate Q_β values relevant for the β -decays, they do not affect the β -decay rates because the half-lives are already experimentally known. Thus, the visi-

ble shifts in the abundance distribution are entirely due to the influence of the new masses on the recalculated neutron-capture rates, which changed by 10-25%. The neutron-capture rates depend on neutron separation energies but also on the choice of the neutron-capture code. Therefore, these calculations done with the TALYS code should be taken as a representative example of the effect of the new mass values on the r -process abundances. However, it can be expected that the effect of the revised neutron separation energies plotted in Fig. 5 would be rather similar even if a different code was used. As can be seen from Fig. 5, the experimental neutron separation energies are systematically lower at $N = 98, 100$ and 102 , leading to smaller odd-even staggering than predicted by the theoretical models. While there were already some indications of overestimated even- N S_n values from previous measurements in the Tb, Gd, and Sm chains, these were single cases in their respective chains. The new data presented in this Letter go further to establish this as a trend, and also extend it to the Pm and Nd chains. Since the odd-even effect is not so pronounced, the final calculated r -process abundances are smoother than what is given by the baseline calculation done with FRDM12. More mass measurements in the region are anticipated to test if the see-saw pattern in the calculated abundances in the heavier mass region is due to the used theoretical mass values.

To fully benefit from new multi-messenger data coming from neutron-star mergers, the precision of r -process calculations needs to be improved with more accurate nuclear data on the involved nuclei. Nuclear binding energies are one of the most crucial inputs for these calculations. In this work, we have determined them for ^{158}Nd , ^{160}Pm , ^{162}Sm , and $^{164-166}\text{Gd}$ for the first time, and improved the precisions for ^{156}Nd , ^{158}Pm , $^{162,163}\text{Eu}$, and ^{164}Tb . Neutron separation energies at $N = 98, 100$ and 102 have been found to be lower than predicted by the theoretical models commonly used in r -process calculations (see Fig. 5). These new data also reveal changes in the slopes of two-neutron separation energies

for the Gd chain at $N = 100$ and for the Nd chain after $N = 96$. The determined two-neutron shell-gap energies do not support the existence of a subshell closure at $N = 100$. This is in agreement with the conclusions made in Refs. [45, 46]. However, the observed features indicate that nuclear structure is changing at these locations, supporting the observations made in Refs. [43, 47].

The r -process abundance pattern in the rare-earth region was investigated for a neutron star merger trajectory. The new mass values yield significant changes of up to 24% in the lanthanide abundances on the lower-mass side of the rare-earth peak. This brought the calculated abundances closer to the solar r -process abundances, which demonstrates the strong influence of these mass measurements on the abundance pattern and highlights the need for accurate mass values in the rare-earth region. This is increasingly important in the era of multi-messenger observations from neutron-star mergers where lanthanides are one of the main indicators of heavy r -process ejecta. The need for accurate nuclear data with which to model and understand the r -process is now greater than ever. Recently developed tools, such as the phase-imaging ion-cyclotron-resonance technique and the multi-reflection time-of-flight mass spectrometer, will prove invaluable in this exploration by facilitating measurements further from stability where low production rates are presently a major impediment.

This work has been supported by the Academy of Finland under the Finnish Centre of Excellence Programme 2012-2017 (Nuclear and Accelerator Based Physics Research at JYFL) and by the National Science Foundation (NSF) Grants No. PHY-1419765 and PHY-1713857. A.K., D.N., and L.C. acknowledge support from the Academy of Finland under project No. 275389. M.M. carried out this work under the auspices of the National Nuclear Security Administration of the U.S. Department of Energy at Los Alamos National Laboratory under Contract No. DE-AC52-06NA25396. R.S. work is funded in part by the DOE Office of Science under contract DE-SC0013039.

-
- [1] E. M. Burbidge, G. R. Burbidge, W. A. Fowler, and F. Hoyle, *Rev. Mod. Phys.* **29**, 547 (1957).
 - [2] A. Cameron, “*Stellar evolution, nuclear astrophysics, and nucleogenesis*,” (1957), Chalk River Report CLR-41. Publisher: Atomic Energy of Canada Limited.
 - [3] M. Arnould, S. Goriely, and K. Takahashi, *Phys. Rep.* **450**, 97 (2007).
 - [4] B. Pfeiffer, K.-L. Kratz, F.-K. Thielemann, and W. Walters, *Nucl. Phys. A* **693**, 282 (2001), radioactive Nuclear Beams.
 - [5] O. Sorlin and M.-G. Porquet, *Progr. Part. Nucl. Phys.* **61**, 602 (2008).
 - [6] J. Erler, N. Birge, M. Kortelainen, W. Nazarewicz, E. Olsen, A. M. Perhac, and M. Stoitsov, *Nature* **486**, 509 (2012).
 - [7] D. Martin, A. Arcones, W. Nazarewicz, and E. Olsen, *Phys. Rev. Lett.* **116**, 121101 (2016).
 - [8] A. Wallner, T. Faestermann, J. Feige, C. Feldstein, K. Knie, G. Korschinek, W. Kutschera, A. Ofan, M. Paul, F. Quinto, G. Rugel, and P. Steier, *Nature Comm.* **6**, 5956 (2015).
 - [9] A. P. Ji, A. Frebel, A. Chiti, and J. D. Simon, *Nature* **531**, 610 (2016).
 - [10] I. U. Roederer, M. Mateo, J. I. B. III, Y. Song, E. F. Bell, J. D. Crane, S. Loebman, D. L. Nidever, E. W. Olszewski, S. A. Sackett, I. B. Thompson, M. Valluri, and M. G. Walker, *Astronom. J.* **151**, 82 (2016).
 - [11] A. Arcones and F.-K. Thielemann, *J. Phys. G: Nucl. Part. Phys.* **40**, 013201 (2013).
 - [12] P. Mösta, C. D. Ott, D. Radice, L. F. Roberts, E. Schnetter, and R. Haas, *Nature* **528**, 376 (2015).
 - [13] J. M. Lattimer and D. N. Schramm, *Astrophys. J. Lett.*

- 192, L145 (1974).**
- [14] D. Argast, M. Samland, F.-K. Thielemann, and Y.-Z. Qian, *Astron. Astrophys.* **416**, 997 (2004), [astro-ph/0309237](https://arxiv.org/abs/astro-ph/0309237).
 - [15] C. Freiburghaus, S. Rosswog, and F.-K. Thielemann, *Astrophys. J. Lett.* **525**, L121 (1999).
 - [16] S. Goriely, A. Bauswein, and H.-T. Janka, *Astrophys. J. Lett.* **738**, L32 (2011).
 - [17] S. Goriely, J.-L. Sida, J.-F. Lemaître, S. Panebianco, N. Dubray, S. Hilaire, A. Bauswein, and H.-T. Janka, *Phys. Rev. Lett.* **111**, 242502 (2013).
 - [18] F.-K. Thielemann, M. Eichler, I. Panov, and B. Wehmeyer, *Annu. Rev. Nucl. Part. Sci.* **67**, 253 (2017), <https://doi.org/10.1146/annurev-nucl-101916-123246>.
 - [19] B. P. Abbott *et al.*, *Astrophys. J. Lett.* **848**, L12 (2017).
 - [20] B. P. Abbott (LIGO Scientific Collaboration and Virgo Collaboration), *Phys. Rev. Lett.* **119**, 161101 (2017).
 - [21] I. Arcavi, G. Hosseinzadeh, D. A. Howell, C. McCully, D. Poznanski, D. Kasen, J. Barnes, M. Zaltzman, S. Vasylyev, D. Maoz, and S. Valenti, *Nature* (2017), <https://doi.org/10.1038/nature24291>.
 - [22] M. M. Kasliwal, E. Nakar, L. P. Singer, D. L. Kaplan, D. O. Cook, A. Van Sistine, R. M. Lau, C. Fremling, O. Gottlieb, J. E. Jencson, S. M. Adams, U. Feindt, K. Hotokezaka, S. Ghosh, D. A. Perley, P.-C. Yu, T. Piran, J. R. Allison, G. C. Anupama, A. Balasubramanian, K. W. Bannister, J. Bally, J. Barnes, S. Barway, E. Bellm, V. Bhalerao, D. Bhattacharya, N. Blagorodnova, J. S. Bloom, P. R. Brady, C. Cannella, D. Chatterjee, S. B. Cenko, B. E. Cobb, C. Copperwheat, A. Corsi, K. De, D. Dobie, S. W. K. Emery, P. A. Evans, O. D. Fox, D. A. Frail, C. Frohmaier, A. Goobar, G. Hallinan, F. Harrison, G. Helou, T. Hinderer, A. Y. Q. Ho, A. Horesh, W.-H. Ip, R. Itoh, D. Kasen, H. Kim, N. P. M. Kuin, T. Kupfer, C. Lynch, K. Madsen, P. A. Mazzali, A. A. Miller, K. Mooley, T. Murphy, C.-C. Ngeow, D. Nichols, S. Nissanke, P. Nugent, E. O. Ofek, H. Qi, R. M. Quimby, S. Rosswog, F. Rusu, E. M. Sadler, P. Schmidt, J. Sollerman, I. Steele, A. R. Williamson, Y. Xu, L. Yan, Y. Yatsu, C. Zhang, and W. Zhao, *Science* (2017), [10.1126/science.aap9455](https://doi.org/10.1126/science.aap9455).
 - [23] D. Kasen, B. Metzger, J. Barnes, E. Quataert, and E. Ramirez-Ruiz, *Nature* (2017), <https://doi.org/10.1038/nature24453>.
 - [24] N. R. Tanvir, A. J. Levan, C. González-Fernández, O. Korobkin, I. Mandel, S. Rosswog, J. Hjorth, P. D’Avanzo, A. S. Fruchter, C. L. Fryer, T. Kangas, B. Milvang-Jensen, S. Rosetti, D. Steeghs, R. T. Wollaeger, Z. Cano, C. M. Copperwheat, S. Covino, V. D’Elia, A. de Ugarte Postigo, P. A. Evans, W. P. Even, S. Fairhurst, R. F. Jaimes, C. J. Fontes, Y. I. Fujii, J. P. U. Fynbo, B. P. Gompertz, J. Greiner, G. Hodosan, M. J. Irwin, P. Jakobsson, U. G. Jørgensen, D. A. Kann, J. D. Lyman, D. Malesani, R. G. McMahon, A. Melandri, P. T. O’Brien, J. P. Osborne, E. Palazzi, D. A. Perley, E. Pian, S. Piranomonte, M. Rabus, E. Rol, A. Rowlinson, S. Schulze, P. Sutton, C. C. Thöne, K. Ulaczyk, D. Watson, K. Wiersema, and R. A. M. J. Wijers, *Astrophys. J. Lett.* **848**, L27 (2017).
 - [25] P. S. Cowperthwaite, E. Berger, V. A. Villar, B. D. Metzger, M. Nicholl, R. Chornock, P. K. Blanchard, W. Fong, R. Margutti, M. Soares-Santos, K. D. Alexander, S. Allam, J. Annis, D. Brout, D. A. Brown, R. E. Butler, H.-Y. Chen, H. T. Diehl, Z. Doctor, M. R. Drout, T. Eftekhari, B. Farr, D. A. Finley, R. J. Foley, J. A. Frieman, C. L. Fryer, J. García-Bellido, M. S. S. Gill, J. Guillochon, K. Herner, D. E. Holz, D. Kasen, R. Kessler, J. Marriner, T. Matheson, E. H. N. Jr., E. Quataert, A. Palmese, A. Rest, M. Sako, D. M. Scolnic, N. Smith, D. L. Tucker, P. K. G. Williams, E. Balbinot, J. L. Carlin, E. R. Cook, F. Durret, T. S. Li, P. A. A. Lopes, A. C. C. Lourenço, J. L. Marshall, G. E. Medina, J. Muir, R. R. Muñoz, M. Sauseda, D. J. Schlegel, L. F. Secco, A. K. Vivas, W. Wester, A. Zenteno, Y. Zhang, T. M. C. Abbott, M. Banerji, K. Bechtol, A. Benoit-Lévy, E. Bertin, E. Buckley-Geer, D. L. Burke, D. Capozzi, A. C. Rosell, M. C. Kind, F. J. Castander, M. Crocce, C. E. Cunha, C. B. D’Andrea, L. N. da Costa, C. Davis, D. L. DePoy, S. Desai, J. P. Dietrich, A. Drlica-Wagner, T. F. Eifler, A. E. Evrard, E. Fernandez, B. Flaugher, P. Fosalba, E. Gaztanaga, D. W. Gerdes, T. Giannantonio, D. A. Goldstein, D. Gruen, R. A. Gruendl, G. Gutierrez, K. Honscheid, B. Jain, D. J. James, T. Jeltema, M. W. G. Johnson, M. D. Johnson, S. Kent, E. Krause, R. Kron, K. Kuehn, N. Kuropatkin, O. Lahav, M. Lima, H. Lin, M. A. G. Maia, M. March, P. Martini, R. G. McMahon, F. Menanteau, C. J. Miller, R. Miquel, J. J. Mohr, E. Neilsen, R. C. Nichol, R. L. C. Ogando, A. A. Plazas, N. Roe, A. K. Romer, A. Roodman, E. S. Rykoff, E. Sanchez, V. Scarpine, R. Schindler, M. Schubnell, I. Sevilla-Noarbe, M. Smith, R. C. Smith, F. Sobreira, E. Suchyta, M. E. C. Swanson, G. Tarle, D. Thomas, R. C. Thomas, M. A. Troxel, V. Vikram, A. R. Walker, R. H. Wechsler, J. Weller, B. Yanny, and J. Zuntz, *Astrophys. J. Lett.* **848**, L17 (2017).
 - [26] A. Aprahamian, I. Bentley, M. Mumpower, and R. Surman, *AIP Advances* **4**, 041101 (2014).
 - [27] S. Brett, I. Bentley, N. Paul, R. Surman, and A. Aprahamian, *Eur. Phys. J. A* **48**, 184 (2012).
 - [28] M. Mumpower, R. Surman, G. McLaughlin, and A. Aprahamian, *Progr. Part. Nucl. Phys.* **86**, 86 (2016).
 - [29] M. R. Mumpower, G. C. McLaughlin, R. Surman, and A. W. Steiner, *J. Phys. G: Nucl. Part. Phys.* **44**, 034003 (2017).
 - [30] P. Möller, A. Sierk, T. Ichikawa, and H. Sagawa, *At. Data Nucl. Data Tables* **109–110**, 1 (2016).
 - [31] S. Goriely, N. Chamel, and J. M. Pearson, *Phys. Rev. C* **88**, 024308 (2013).
 - [32] J. Duflo and A. Zuker, *Phys. Rev. C* **52**, R23 (1995).
 - [33] M. Wang, G. Audi, F. Kondev, W. Huang, S. Naimi, and X. Xu, *Chin. Phys. C* **41**, 030003 (2017).
 - [34] R. Surman, J. Engel, J. R. Bennett, and B. S. Meyer, *Phys. Rev. Lett.* **79**, 1809 (1997).
 - [35] M. R. Mumpower, G. C. McLaughlin, and R. Surman, *Phys. Rev. C* **85**, 045801 (2012).
 - [36] J. Beun, G. C. McLaughlin, R. Surman, and W. R. Hix, *Phys. Rev. C* **77**, 035804 (2008).
 - [37] K. Lodders, H. Palme, and H.-P. Gail, “4.4 Abundances of the elements in the Solar System: Datasheet from Landolt-Börnstein - Group VI Astronomy and Astrophysics · Volume 4B: “Solar System” in SpringerMaterials (http://dx.doi.org/10.1007/978-3-540-88055-4_34),” (2009), accessed 2017-07-18.
 - [38] P. Brix, *Z. Phys.* **132**, 579 (1952).
 - [39] B. R. Mottelson and S. G. Nilsson, *Phys. Rev.* **99**, 1615 (1955).
 - [40] R. F. Casten, D. D. Warner, D. S. Brenner, and R. L.

- Gill, *Phys. Rev. Lett.* **47**, 1433 (1981).
- [41] D. Bonatsos, S. Karampagia, R. B. Cakirli, R. F. Casten, K. Blaum, and L. A. Susam, *Phys. Rev. C* **88**, 054309 (2013).
- [42] R. Casten, *Nat. Phys.* **2**, 811 (2006).
- [43] E. F. Jones, J. H. Hamilton, P. M. Gore, A. V. Ramayya, J. K. Hwang, and A. P. deLima, *Eur. Phys. J. A* **25**, 467 (2005).
- [44] S. K. Ghorui, B. B. Sahu, C. R. Praharaj, and S. K. Patra, *Phys. Rev. C* **85**, 064327 (2012).
- [45] J. Wu, S. Nishimura, G. Lorusso, P. Möller, E. Ideguchi, P.-H. Regan, G. S. Simpson, P.-A. Söderström, P. M. Walker, H. Watanabe, Z. Y. Xu, H. Baba, F. Browne, R. Daido, P. Doornenbal, Y. F. Fang, G. Gey, T. Isobe, P. S. Lee, J. J. Liu, Z. Li, Z. Korkulu, Z. Patel, V. Phong, S. Rice, H. Sakurai, L. Sinclair, T. Sumikama, M. Tanaka, A. Yagi, Y. L. Ye, R. Yokoyama, G. X. Zhang, T. Alharbi, N. Aoi, F. L. Bello Garrote, G. Benzoni, A. M. Bruce, R. J. Carroll, K. Y. Chae, Z. Dombradi, A. Estrade, A. Gottardo, C. J. Griffin, H. Kanaoka, I. Kojouharov, F. G. Kondev, S. Kubono, N. Kurz, I. Kuti, S. Lalkovski, G. J. Lane, E. J. Lee, T. Lokotko, G. Lotay, C.-B. Moon, H. Nishibata, I. Nishizuka, C. R. Nita, A. Odahara, Z. Podolyák, O. J. Roberts, H. Schaffner, C. Shand, J. Taproge, S. Terashima, Z. Vajta, and S. Yoshida, *Phys. Rev. Lett.* **118**, 072701 (2017).
- [46] R. Yokoyama, S. Go, D. Kameda, T. Kubo, N. Inabe, N. Fukuda, H. Takeda, H. Suzuki, K. Yoshida, K. Kusaka, K. Tanaka, Y. Yanagisawa, M. Ohtake, H. Sato, Y. Shimizu, H. Baba, M. Kurokawa, D. Nishimura, T. Ohnishi, N. Iwasa, A. Chiba, T. Yamada, E. Ideguchi, T. Fujii, H. Nishibata, K. Ieki, D. Murai, S. Momota, Y. Sato, J. W. Hwang, S. Kim, O. B. Tarasov, D. J. Morrissey, B. M. Sherrill, G. Simpson, and C. R. Praharaj, *Phys. Rev. C* **95**, 034313 (2017).
- [47] Z. Patel, P.-A. Söderström, Z. Podolyák, P. H. Regan, P. M. Walker, H. Watanabe, E. Ideguchi, G. S. Simpson, H. L. Liu, S. Nishimura, Q. Wu, F. R. Xu, F. Browne, P. Doornenbal, G. Lorusso, S. Rice, L. Sinclair, T. Sumikama, J. Wu, Z. Y. Xu, N. Aoi, H. Baba, F. L. Bello Garrote, G. Benzoni, R. Daido, Y. Fang, N. Fukuda, G. Gey, S. Go, A. Gottardo, N. Inabe, T. Isobe, D. Kameda, K. Kobayashi, M. Kobayashi, T. Komatsubara, I. Kojouharov, T. Kubo, N. Kurz, I. Kuti, Z. Li, M. Matsushita, S. Michimasa, C.-B. Moon, H. Nishibata, I. Nishizuka, A. Odahara, E. Şahin, H. Sakurai, H. Schaffner, H. Suzuki, H. Takeda, M. Tanaka, J. Taproge, Z. Vajta, A. Yagi, and R. Yokoyama, *Phys. Rev. Lett.* **113**, 262502 (2014).
- [48] J. Van Schelt, D. Lascar, G. Savard, J. A. Clark, S. Caldwell, A. Chaudhuri, J. Fallis, J. P. Greene, A. F. Levand, G. Li, K. S. Sharma, M. G. Sternberg, T. Sun, and B. J. Zabransky, *Phys. Rev. C* **85**, 045805 (2012).
- [49] H. Hayashi, M. Shibata, M. Asai, A. Osa, T. Sato, M. Koizumi, A. Kimura, and M. Oshima, *Nucl. Instrum. Methods Phys. Res. Sect. A* **747**, 41 (2014).
- [50] J. Äystö, *Nucl. Phys. A* **693**, 477 (2001).
- [51] P. Karvonen, I. Moore, T. Sonoda, T. Kessler, H. Penttilä, K. Peräjärvi, P. Ronkanen, and J. Äystö, *Nucl. Instrum. Methods Phys. Res. Sect. B* **266**, 4794 (2008).
- [52] A. Nieminen, J. Huikari, A. Jokinen, J. Äystö, P. Campbell, and E. Cochrane, *Nucl. Instrum. Methods Phys. Res. Sect. A* **469**, 244 (2001).
- [53] T. Eronen, V. S. Kolhinen, V. V. Elomaa, D. Gorelov, U. Hager, J. Hakala, A. Jokinen, A. Kankainen, P. Karvonen, S. Kopecky, I. D. Moore, H. Penttilä, S. Rahaman, S. Rinta-Antila, J. Rissanen, A. Saastamoinen, J. Szerypo, C. Weber, and J. Äystö, *Eur. Phys. J. A* **48**, 46 (2012).
- [54] G. Savard, S. Becker, G. Bollen, H. J. Kluge, R. B. Moore, T. Otto, L. Schweikhard, H. Stolzenberg, and U. Wiess, *Phys. Lett. A* **158**, 247 (1991).
- [55] T. Eronen, V.-V. Elomaa, U. Hager, J. Hakala, A. Jokinen, A. Kankainen, S. Rahaman, J. Rissanen, C. Weber, and J. Äystö, *Nucl. Instrum. Methods Phys. Res. Sect. B* **266**, 4527 (2008).
- [56] G. Gräff, H. Kalinowsky, and J. Traut, *Z. Phys. A* **297**, 35 (1980).
- [57] M. König, G. Bollen, H. J. Kluge, T. Otto, and J. Szerypo, *Int. J. Mass Spectrom. Ion Processes* **142**, 95 (1995).
- [58] M. Kretzschmar, *Int. J. Mass Spectrom.* **264**, 122 (2007).
- [59] S. George, K. Blaum, F. Herfurth, A. Herlert, M. Kretzschmar, S. Nagy, S. Schwarz, L. Schweikhard, and C. Yazidjian, *Int. J. Mass Spectrom.* **264**, 110 (2007).
- [60] C. Weber, V.-V. Elomaa, R. Ferrer, C. Fröhlich, D. Ackermann, J. Äystö, G. Audi, L. Batist, K. Blaum, M. Block, A. Chaudhuri, M. Dworschak, S. Eliseev, T. Eronen, U. Hager, J. Hakala, F. Herfurth, F. P. Heßberger, S. Hofmann, A. Jokinen, A. Kankainen, H.-J. Kluge, K. Langanke, A. Martín, G. Martínez-Pinedo, M. Mazzocco, I. D. Moore, J. B. Neumayr, Y. N. Novikov, H. Penttilä, W. R. Plaß, A. V. Popov, S. Rahaman, T. Rauscher, C. Rauth, J. Rissanen, D. Rodríguez, A. Saastamoinen, C. Scheidenberger, L. Schweikhard, D. M. Seliverstov, T. Sonoda, F.-K. Thielemann, P. G. Thirolf, and G. K. Vorobjev, *Phys. Rev. C* **78**, 054310 (2008).
- [61] L. Canete, A. Kankainen, T. Eronen, D. Gorelov, J. Hakala, A. Jokinen, V. S. Kolhinen, J. Koponen, I. D. Moore, J. Reinikainen, and S. Rinta-Antila, *Eur. Phys. J. A* **52**, 124 (2016).
- [62] J. Shergur, B. A. Brown, V. Fedoseyev, U. Köster, K.-L. Kratz, D. Seweryniak, W. B. Walters, A. Wöhr, D. Fedorov, M. Hannawald, M. Hjorth-Jensen, V. Mishin, B. Pfeiffer, J. J. Ressler, H. O. U. Fynbo, P. Hoff, H. Mach, T. Nilsson, K. Wilhelmsen-Rolander, H. Simon, A. Bickley, and ISOLDE Collaboration, *Phys. Rev. C* **65**, 034313 (2002).
- [63] S. Gujrathi and J. D’auria, *Nucl. Phys. A* **172**, 353 (1971).
- [64] W. Huang, G. Audi, M. Wang, F. Kondev, S. Naimi, and X. Xu, *Chin. Phys. C* **41**, 030002 (2017).
- [65] D. Lunney, J. M. Pearson, and C. Thibault, *Rev. Mod. Phys.* **75**, 1021 (2003).
- [66] U. Hager, T. Eronen, J. Hakala, A. Jokinen, V. S. Kolhinen, S. Kopecky, I. Moore, A. Nieminen, M. Oinonen, S. Rinta-Antila, J. Szerypo, and J. Äystö, *Phys. Rev. Lett.* **96**, 042504 (2006).
- [67] L. Satpathy and S. Patra, *Nucl. Phys. A* **722**, C24 (2003).
- [68] L. Satpathy and S. K. Patra, *J. Phys. G: Nucl. Part. Phys.* **30**, 771 (2004).
- [69] G. Audi, F. Kondev, M. Wang, W. Huang, and S. Naimi, *Chin. Phys. C* **41**, 030001 (2017).
- [70] P. Möller, B. Pfeiffer, and K.-L. Kratz, *Phys. Rev. C* **67**, 055802 (2003).
- [71] A. Koning and D. Rochman, *Nucl. Data Sheets* **113**, 2841

- (2012), special Issue on Nuclear Reaction Data.
- [72] O. Just, A. Bauswein, R. A. Pulpillo, S. Goriely, and H.-T. Janka, *Mon. Not. R. Astron. Soc.* **448**, 541 (2015), [arXiv:1406.2687 \[astro-ph.SR\]](#).